Operation of a Tube GAHE in Northeastern Poland in Spring and Summer—A Comparison of Real-World Data with Mathematically Modeled Data

Aldona Skotnicka-Siepsiak [ID]

Faculty of Geoengineering, University of Warmia and Mazury in Olsztyn, 10-724 Olsztyn, Heweliusza, Poland; aldona.skotnicka-siepsiak@uwm.edu.pl

Abstract: The article analyzes a ground-to-air heat exchanger (GAHE) for a mechanical ventilation system in a building. The heat exchanger's performance was evaluated in northeastern Poland between May and August of 2016, 2017, and 2018. In spring and summer, the GAHE can be theoretically used to precool air for HVAC systems. The aim of the study was to compare the real-world performance of GAHE with its theoretical performance determined based on the distribution of ground temperature and the temperature at the GAHE outlet modeled in compliance with Standard PN-EN 16798-5 1:2017-07. The modeled values differed considerably from real-world data in May and June, but the model demonstrated satisfactory data fit in July and August. In all years, the modeled average monthly air temperature at the GAHE outlet was 8.3 °C below real-world values in May, but the above difference was only 1.1 °C in August. The developed mathematical model is simple and easy to use, and it can be deployed already in the preliminary design stage. It does not require expensive software or expert skills. However, this study revealed that the model has several limitations. The observed discrepancies should be taken into account when modeling the performance of a GAHE.

Keywords: ground-to-air heat exchangers; GAHE; experimental results; preheating and precooling for HVAC; energy saving for HVAC; models for calculating the thermal efficiency of ground-to-air heat exchangers

1. Introduction

A ground-to-air heat exchanger (GAHE) is a relatively simple technology which can be incorporated with conventional heating, ventilation, and air-conditioning (HVAC) installations to preheat and precool air [1]. Despite its simplicity, a GAHE can effectively lower the demand for indoor heat and minimize the environmental impact of heating installations [2].

In Poland, GAHEs are increasingly often used to preheat air, both in small ventilation systems in single-family homes and in large installations where the diameter of ground tubes exceeds 900 mm [3]. The performance of a GAHE in the winter of 2016 was analyzed by [4]. The experimentally measured values were compared with theoretical computational models based on Standard PN-EN 15241:2011 [5,6]. A comparison of outdoor air temperature measured experimentally at the GAHE outlet with the modeled data revealed that the average monthly heating load was 23% higher in the theoretical model. Even greater discrepancies were observed when typical meteorological year (TMY) data were used in the calculations, where the average heat gain was 34% higher in the model than in the experimental measurements. These differences can be attributed mainly to the fact that the temperatures of outdoor air in the TMY dataset were significantly below the measured temperatures, in particular in winter. This observation is not surprising in the face of global climate change.

A GAHE can also be used to precool air, and such applications have been analyzed in research studies conducted in Iraq [7], India [8], Algeria [9], China [10], and Turkey [11]. However, not only sensible heat transfer—but also latent heat exchange—has to be taken into account when air precooled in a GAHE is fed to HVAC installations [12].

The GAHE concept and design continues to be studied, optimized and developed. The current state of knowledge and the most recent developments have been presented in several review articles [13–15]. Some authors have investigated selected aspects of GAHE design and operation. Misra et al. [16] proposed a solution for minimizing GAHE installation costs and maximizing energy gain. Baglivo et al. [17] aimed to determine the optimal number of tubes in a horizontal GAHE by analyzing air temperature, air flow rate, pipe depth, and soil thermal conductivity in TRNSYS 17 software. GAHEs can be integrated with solar chimneys for passive cooling of buildings [18].

The operation, design, and optimization of GAHEs are often analyzed with the use of numerical simulations [19–21]. Kumar et al. [22] relied on a genetic algorithm to optimize the design of a GAHE. The authors compared a deterministic model with an intelligent design model. The intelligent model, which accounted for variations in the humidity of circulating air, natural thermal stratification of the ground, latent and sensible heat transfer, as well as ground conditions, proved to be a more effective solution. Ahmed et al. [23] used the Fluent software package to develop a model for the Australian climate which revealed that the cooling load of a GAHE can be optimized by increasing the depth at which the tubes are buried in the ground, maximizing the tubes' thermal conductivity, and minimizing tube diameter and the thickness of tube walls. The optimal air flow rate in the analyzed system was 1.5 m/s. Rodrigues et al. [24] relied on the constructal design method to optimize the thermal capacity of a GAHE. Bisoniya [25] described the application of the ε-NTU method for designing an effective GAHE installation. Rouag, Benchabane, and Mehdid [26,27] developed a semi-analytical method to determine the distance from the pipe axis in the ground (soil radius) influenced by heat from the GAHE. Unlike other researchers, the authors assumed that the soil radius affected by heat from the GAHE is not stable and that it is influenced by the duration of operation, soil thermal diffusivity, pipe diameter, and air temperature.

Despite the availability of numerous CFD methods, there is a demand for simple computational models for engineers who do not have access to advanced numerical tools. A simple method for estimating the preheating and precooling requirements of a HVAC installation coupled to a GAHE has been proposed by Chiesa [28]. In the cited study, the model's effectiveness was evaluated with the use of three key performance indicators (KPI): an analysis of the number of operating hours based on a psychrometric chart, the anticipated sensible heat exchange (in winter and summer), and the determination of a virtual coefficient of performance based on a theoretically calculated pressure drop. Peretti et al. [29] discussed the design and environmental impacts of a GAHE in a review article. The authors reviewed the existing models and algorithms for evaluating heat transfer in soil and the thermal behavior of pipes, and they discussed several real-world applications of GAHEs. The article presents formulas for determining the heating and cooling loads of a GAHE, including formulas for calculating the interactions between ground and ambient air, heat transfer equations, and a mathematical model for determining the annual subsurface soil temperature. Peretti applied a mathematical model of ground temperature developed by [30]. Other mathematical models have been proposed by ASHRAE [31]; Tittelein, Achard, and Wurtz [32]; Badache et al. [33]; and Ozgener, Ozgener, and Tester [34]. An empirical model for calculating soil temperature was described by Popiel and Wojtkowiak [6].

The aim of this study was to compare the real-world performance and the theoretical performance of a GAHE based on the results of an experiment and a mathematical model developed in accordance with Standard PN-EN 16798-5 1:2017-07 "*Energy Performance of Buildings—Ventilation for Buildings—Part 5-1: Calculation Methods for Energy Requirements of Ventilation and Air Conditioning Systems (Modules M5-6, M5-8, M6-5, M6-8, M7-5, M7-8)—Method 1: Distribution and Generation*". The experimental setup for real-world measurements is presented in the next section. The mechanical ventilation system in

the presented experiment supported both air precooling and preheating. The mathematical model was developed based on Standard PN-EN 16798-5 1:2017-07 to determine temperature distribution in the ground. The above standard was also applied to calculate air temperature at the GAHE outlet (the temperature of outdoor air was determined based on TMY data and the measurements conducted in the summers of 2016, 2017, and 2018). The modeled data were compared with the results of the experimental measurements of GAHE performance.

2. Materials and Methods

Laboratory analyses were carried out in the Institute of Civil Engineering of the University of Warmia and Mazury in Olsztyn (Poland). The experimental setup involved an AwaduktThermo ground-to-air heat exchanger (GAHE) buried in the ground to a depth of 1.97 m at a point where the tube crossed the wall of a building to 2.27 m by a water drainage tank. The experimental setup is presented graphically in Figure 1. The tubes were buried in the ground (wet sand) with a downward slope in the direction of the water drainage tank located in the proximity of the AwaduktThermo air intake stack. Total tube length was 41 m, and internal tube diameter was 0.2 m.
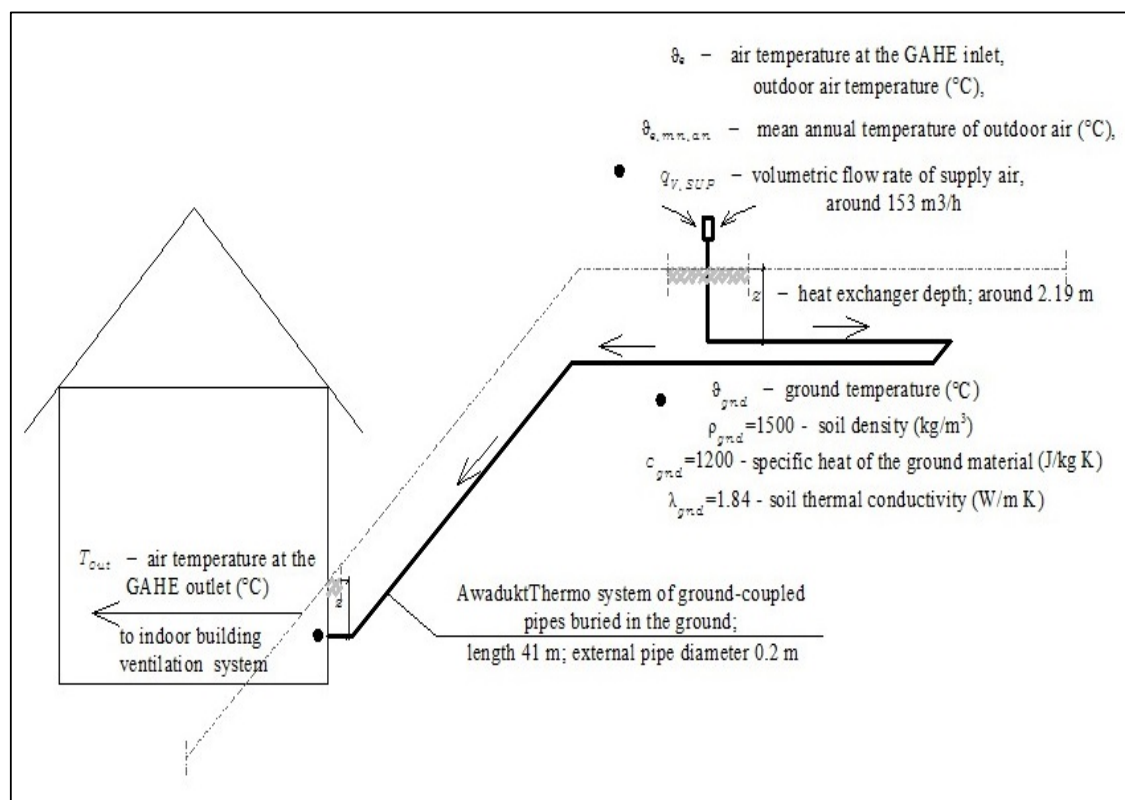

Figure 1. Diagram of the experimental setup.

AwaduktThermo tubes were the main element of the experimental setup. The tubes have antibacterial internal lining, and the base polymer is enhanced with silver particles to reduce microbial contamination in the system. The antibacterial properties of internal tube lining have been tested and certified by the Polish National Institute of Public Health and Institut Fresenius in Taunusstein, Germany. The tubes have solid polypropylene walls for optimal heat transfer [35].

The measurements were conducted with resistance temperature detectors and humidity sensors installed outdoors and in the GAHE at the point where the tubes entered the building. Temperature at the GAHE inlet and outlet was measured with the Siemens QAM2120.040 duct temperature sensor with a measuring range of $-50\,°\text{C}$ to $+80\,°\text{C}$. The resistance of the sensing element changes as a function of temperature, and measuring accuracy is ± 0.4 K at $0\,°\text{C}$ and ± 0.5 K at $20\,°\text{C}$. The device is equipped

with an LG-Ni 1000 sensing element with a nominal resistance of 1000 Ω/0 °C, and it has a time constant of less than 20 s during assembly in a pipeline. Humidity was measured with the Siemens QFM2100 duct sensor with a measuring range of 0% to 100%, and measuring accuracy of ±5% at 23 °C and 24 V AC. Air flow meters were installed in the GAHE, and a pyranometer was also used. The pyranometer has a spectral range of 300 nm to 2800 nm, output voltage of 5 mV/W/m² to 20 mV/W/m², response time of 18 s, and directional error of less than 20 W/m². The air flow rate was determined with the Siemens QVM62.1 air velocity sensor with a measuring range of 0 to 10 m/s and measuring accuracy of ±0.2 m/s (+3% of the measured value) at 20 °C, 45% humidity, and atmospheric pressure of 1013 hPa. Sensor data were registered by a Siemens controller in real time and were averaged at hourly intervals.

The measurements were conducted between May and August of 2016, 2017, and 2018. Meteorological data were compared with typical meteorological year (TMY) data, and 2952 measurements were obtained in every analyzed year. The number of measurements conducted at the GAHE outlet was determined by the system's operating time (Figure 2). In 2016, the GAHE operated continuously (2952 h), and the average air flow rate was approximately 163 m³/h. In the remaining years of the experiment, the GAHE operated intermittently. In May 2017, the system operated at weekly intervals. In June 2017, three operating days were followed by a five-day pause. In July and August 2017, the GAHE operated on working days only, for around 8 h per day (7:00 a.m. to 3:00 p.m.). In 2018, the GAHE operated continuously in May and in the first half of June. Between mid-June and mid-July 2018, the system operated intermittently at 7-day to 14-day intervals. From mid-July to the end of August 2018, the GAHE operated on working days only, for around 8 h per day (7:00 a.m. to 3:00 p.m.). In 2017, total operating time was 1038 h with an average air flow rate of around 150 m³/h. In 2018, total operating time was 1608 h with an average air flow rate of around 145 m³/h.
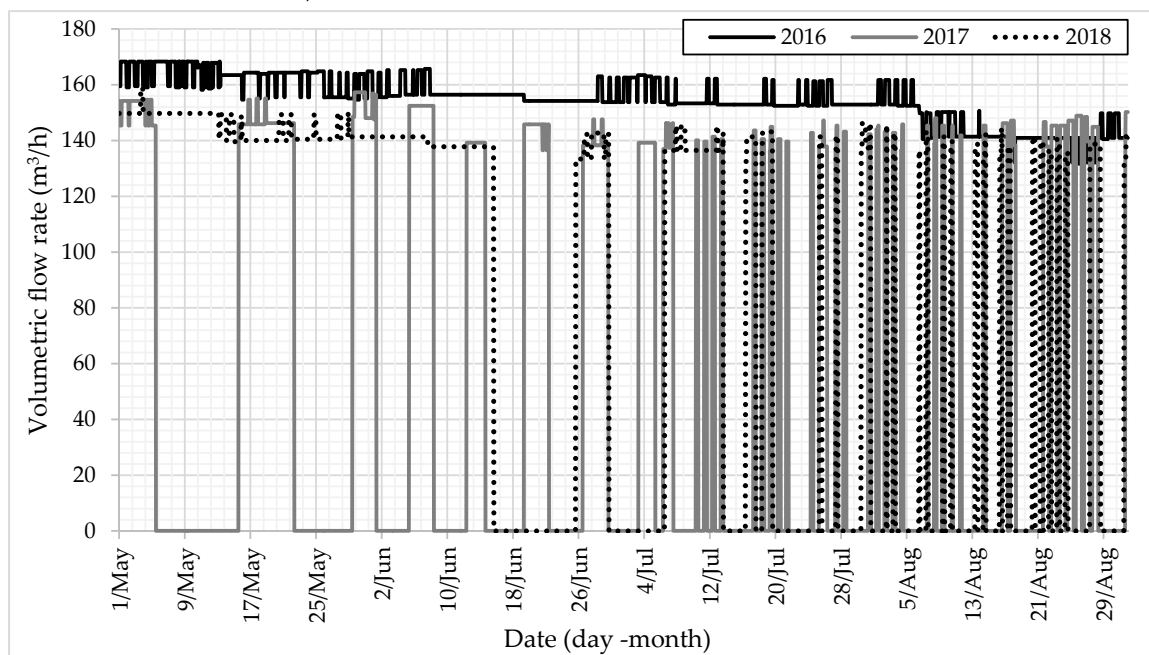

Figure 2. GAHE operating time.

The heating and cooling loads of the GAHE were calculated with the following formula [36]

$$Q = \dot{m} \cdot c_p \cdot (T_{Out} - T_{In}) \tag{1}$$

where:

   Q—heat gain from the GAHE (W);
   $\dot{m}$—mass flow rate of air (kg/s);

c_p—specific heat of air (J/(kg·K));

T_{In}—air temperature at the GAHE inlet (outdoor air) (K);

T_{Out}—air temperature at the GAHE outlet (K).

A positive result indicates that heat was transferred from the ground-to-air, whereas a negative result indicates that air was cooled in the GAHE. Heating and cooling loads were determined on an hourly basis, and the results were expressed in Wh.

However, Equation (1) requires real-world data that have to be obtained through experimental measurements. Air temperature at the GAHE outlet is most difficult to measure at the design stage. The difference in air temperature between the GAHE inlet and outlet can be determined based on Standard PN-EN 16798-5-1:2017-07

$$\Delta\vartheta_{gnd} = \left(\vartheta_{gnd} - \vartheta_e\right)\left[1 - e^{-\left(\frac{U_{du}\cdot A_s}{q_{V;SUP}\rho_a c_a}\right)}\right] \tag{2}$$

where:

ϑ_e—outdoor air temperature (°C);

A_s—inner surface area of the GAHE (m^2);

$q_{V;SUP}$—volumetric flow rate of supply air (m^3/h);

ρ_a—air density (kg/m^3);

c_a—specific heat of air at constant pressure, ($c_a = 0.000279$ kWh/(kg K)).

Ground temperature ϑ_{gnd} is calculated with the formula

$$\vartheta_{gnd} = \vartheta_{e;mn;an} + \left(\vartheta_{e;max;m} - \vartheta_{e;mn;an}\right)\cdot e^{-\xi}\cdot\cos\left(2\pi\cdot\frac{t_{an}}{8760} - \xi - f_t\right) \tag{3}$$

where:

$\vartheta_{e;mn;an}$—mean annual temperature of outdoor air (°C);

$\vartheta_{e;max;m}$—maximum mean monthly temperature of outdoor air (°C);

t_{an}—hours per year (h).

Coefficient ξ accounts for soil type and the depth of GAHE tubes

$$\xi = z\cdot\sqrt{\frac{\pi\cdot\rho_{gnd}\cdot c_{gnd}}{\lambda_{gnd}\cdot 8760\cdot 3600}} \tag{4}$$

where:

ρ_{gnd}—soil density, (1500 kg/m^3);

c_{gnd}—specific heat of the ground material, (1200 J/kg K);

λ_{gnd}—soil thermal conductivity, (1.88 W/m K);

z—tube depth (m).

The flow time coefficient f_t is given by the formula

$$f_t = \pi\left(\frac{2\cdot t_{an;;in}}{8760} + 1\right) \tag{5}$$

where:

$t_{an;min}$—number of hours in the year with minimal mean monthly temperature of outdoor air (h).

The overall heat transfer coefficient of the GAHE is expressed by the formula

$$U_{du} = \left(\frac{1}{2\pi}\cdot\frac{1}{\lambda_{du}}\cdot\ln\frac{\frac{d_o}{2}}{\frac{d_i}{2}} + \frac{1}{h_i}\right)^{-1} \tag{6}$$

where:

λ_{du}—thermal conductivity of the tube, (0.28 W/m K);
d_i—inner diameter of the tube, (0.200 m);
d_o—outer diameter of the tube, (0.188 m).
The inside surface coefficient h_i is calculated as

$$h_i = \left[4.13 + 0.23 \cdot \frac{\vartheta_m}{100} - 0.0077 \cdot \left(\frac{\vartheta_m}{100} \right)^2 \right] \cdot \frac{v^{0.75}}{d_i^{0.25}} \tag{7}$$

where:

ϑ_m—average air temperature inside the tube (°C);
v—air velocity inside the tube (m/s).

Ground temperature and the difference in air temperature between the GAHE inlet and outlet in the analyzed period (May to August 2016, 2017, and 2018) were determined with the use of a theoretical mathematical model compliant with Standard PN-EN 16798-5-1:2017-07 and formulas (2) to (7). The calculations were performed for the measured temperatures of outdoor air and the measured air flow rates in each year of the experiment. The theoretical heating and cooling loads of the GAHE were determined with the use of formula (1). The results produced by the theoretical model were compared with the results of the calculations performed with the use of formula (1) based on the experimentally measured values.

Latent heat transfer, namely the energy released during water vapor condensation, was determined with the use of formula (8) at hourly intervals [37]. The results were expressed in Wh.

$$Q_t = \dot{m} \cdot (h_{Out} - h_{In}) \tag{8}$$

where:

Q_t—latent heat transfer, (W);
$\dot{m}$—mass air flow rate (kg/s);
h_{In}—enthalpy of fresh air at the GAHE inlet (J/kg);
h_{Out}—enthalpy of fresh air at the GAHE outlet (J/kg).
Air enthalpy was calculated with the below formula:

$$h = c_d \cdot t + (q + c_v \cdot t) \cdot d \tag{9}$$

where:

h—air enthalpy (J/kg);
c_d—average specific heat of dry air at constant pressure, (1001 J/(kg K));
t—air temperature (K);
q—vaporization heat of water at 0 °C, (2,500,000 J/kg);
c_v—average specific heat of water vapor at constant pressure, (1840 J/(kg K));
d—specific humidity (kg/kg).

3. Results

Temperatures exceeded TMY values in each year of the study. The average TMY temperature in the analyzed period was 15.1 °C, whereas the average annual temperature during the experiment was determined at 16.6 °C in 2016, 17.0 °C in 2017, and 19.2 °C in 2018 (Figure 3). In the analyzed period, the lowest TMY temperature was −3.2 °C and the highest TMY temperature was 31.0 °C. During the experiment, the corresponding values were determined at 3.4 °C and 32.1 °C in 2016, 0.1 °C and 29.0 °C in 2017, and 4.8 °C and 31.5 °C in 2018. The above trend was also observed in analyses of monthly data.
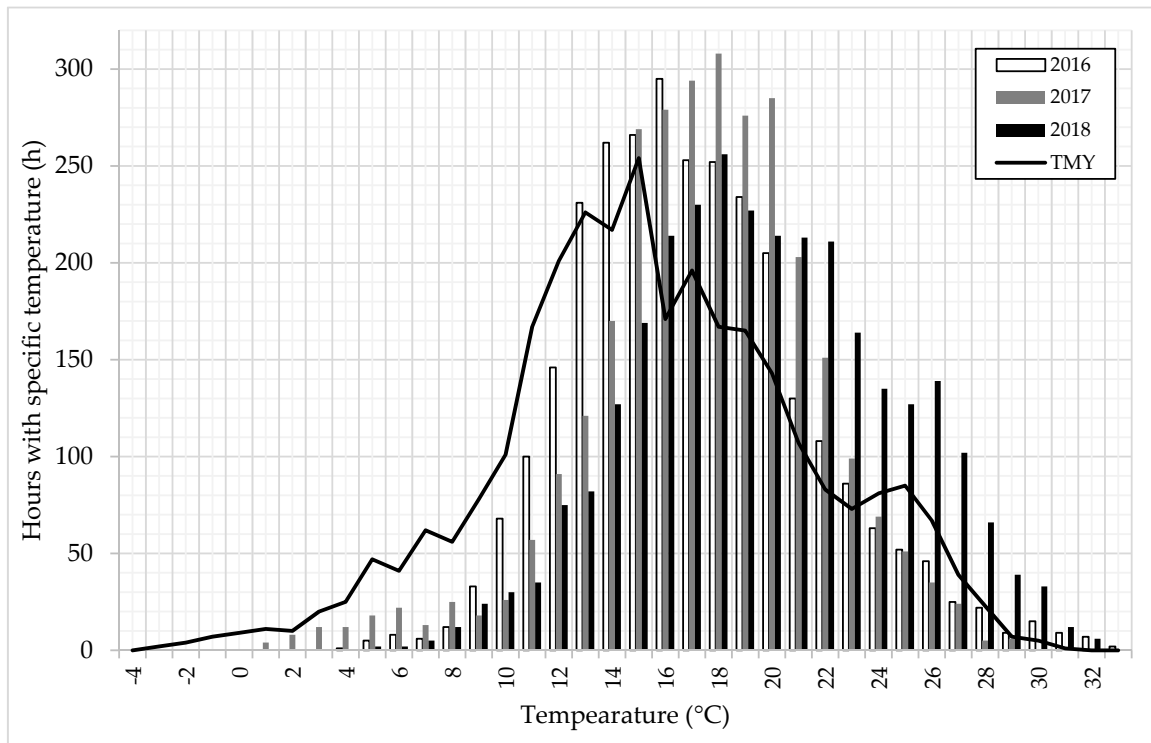
Figure 3. Distribution of outdoor air temperature in the analyzed period.

Total solar irradiance (TSI) in the analyzed period was determined at 515,867 W/m^2 based on TMY data, and the measured values were: 553,801 W/m^2 in 2016, 561,828 W/m^2 in 2017, and 635,253 W/m^2 in 2018. In the TMY dataset, the highest TSI (1040.0 W/m^2) was noted on 20 May at noon. In 2016, maximum TSI was 1182.4 W/m^2 on 16 June at 1:00 p.m. In 2017, the highest TSI (1229.5 W/m^2) was observed on 3 July at 3:00 p.m. In 2018, TSI peaked at 1139.8 W/m^2 on 12 August at 4:00 p.m.

Air temperatures measured at the GAHE outlet and the modeled temperatures are presented in Figure 4.
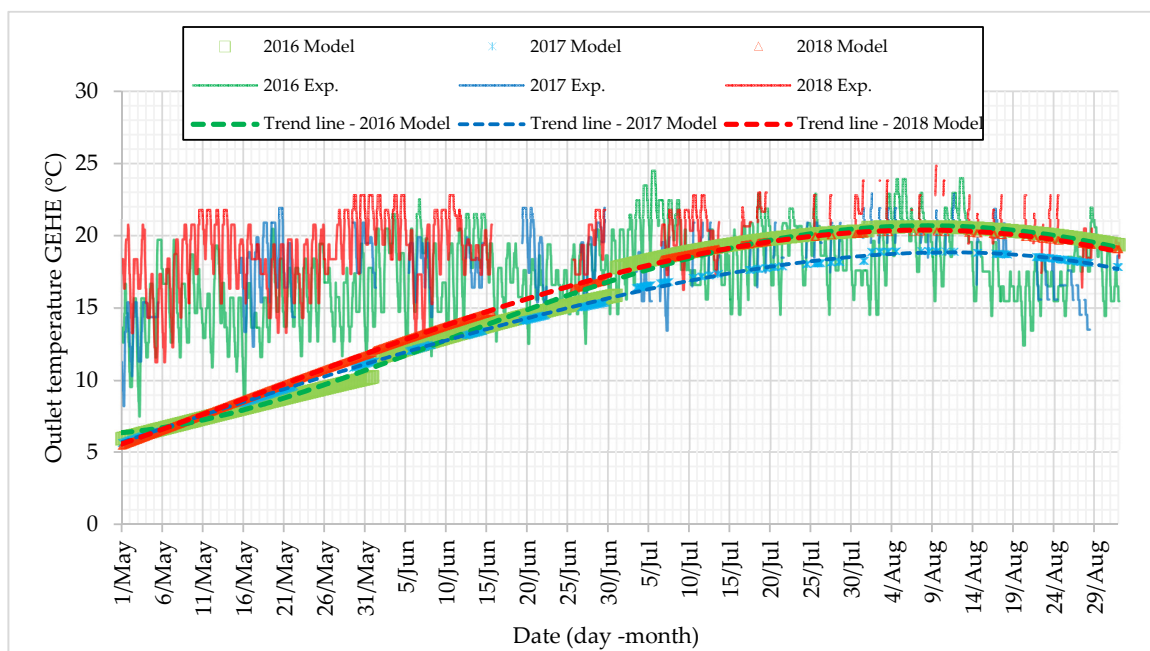

Figure 4. Temperature distribution at the GAHE outlet relative to the modeled temperatures.

The greatest differences between the experimentally measured and the modeled values were noted in the first half of the analyzed period. In May, the average monthly temperature measured at the GAHE outlet was determined at 15.2 °C in 2016, 16.7 °C in 2017, and 18.4 °C in 2018. The corresponding modeled temperatures were 8.1 °C in 2016, 8.4 °C in 2017, and 8.8 °C in 2018. In June 2016, the average monthly temperature measured at the GAHE outlet was 17.6 °C in 2016, 18.4 °C in 2017, and 19.6 °C in 2018. The corresponding data in the model were: 13.8 °C in 2016, 13.7 °C in 2017, and 14.1 °C in 2018. In July 2016, the average monthly temperature measured at the GAHE outlet was 19.2 °C in 2016, 18.6 °C in 2017, and 20.9 °C in 2018. The corresponding values in the model were 19.3 °C in 2016, 17.3 °C in 2017, and 19.1 °C in 2018. In August 2016, the average temperature measured at the GAHE outlet was 18.5 °C in 2016, 18.1 °C in 2017, and 20.8 °C in 2018. The corresponding modeled temperatures were 20.3 °C in 2016, 18.5 °C in 2017, and 19.8 °C in 2018.

Based on an analysis of the hourly differences in temperature between the GAHE inlet and the GAHE outlet (ambient air), the maximum heating load and the maximum cooling load were determined at 4.8 °C and 1.9 °C, respectively, in May 2016; 3.8 °C and 5.6 °C, respectively, in June 2016; 4.0 °C and 7.2 °C, respectively, in July 2016; 4.8 °C and 8.1 °C, respectively, in August 2016. In 2017, the maximum heating load and the maximum cooling load reached 6.4 °C and 4.8 °C, respectively in May; 3.2 °C and 4.7 °C, respectively, in June; 4.5 °C and 3.2 °C, respectively, in July; 3.5 °C and 5.6 °C, respectively, in August. In 2018, the maximum heating load and the maximum cooling load were determined at 6.5 °C and 6.8 °C, respectively in May (Table 1); 6.1 °C and 7.0 °C, respectively, in June; 4.2 °C and 6.4 °C, respectively, in July; 7.1 °C and 6.9 °C, respectively, in August.

Table 1. Distribution of average hourly temperatures measured at the GAHE inlet and outlet

Variable		Year	May	June	July	August
Hourly Ambient Air Temperature (°C)	Max.	2016	22.0	27.4	31.7	32.1
		2017	26.7	26.6	27.9	29.0
		2018	29.6	30.1	31.4	31.5
	Min.	2016	3.4	9.0	11.8	7.9
		2017	0.1	7.6	10.8	11.0
		2018	4.8	7.1	11.6	8.5
	Avg.	2016	13.4	16.8	18.9	17.5
		2017	14.2	17.3	17.9	18.3
		2018	17.4	18.6	20.7	20.2
Hourly Temperature Distribution at the GAHE Outlet (°C)	Max.	2016	20.5	22.5	24.5	24.0
		2017	21.9	21.9	21.9	22.9
		2018	22.8	22.8	23.8	24.8
	Min.	2016	7.5	11.7	14.5	12.4
		2017	8.2	14.4	13.4	13.5
		2018	11.3	13.2	16.3	16.4
	Avg.	2016	15.2	17.6	19.2	18.5
		2017	16.7	18.4	18.6	18.1
		2018	18.4	19.6	20.9	20.8
Hourly Differences in Temperature Between the GAHE Inlet and the GAHE Outlet (°C)	Heating	2016	4.8	3.8	4.0	4.8
		2017	6.4	3.2	4.5	3.5
		2018	6.5	6.1	4.2	7.1
	Cooling	2016	−1.9	−5.6	−7.2	−8.1
		2017	−4.8	−4.7	−3.2	−5.6
		2018	−6.8	−7.0	−6.4	−6.9
	Avg.	2016	1.8	0.8	0.3	1.0
		2017	1.2	0.7	0.8	0.7
		2018	1.0	0.7	0.0	0.3

Table 1. *Cont.*

Variable	Year	May	June	July	August
Total Operating Time (h)	2016	744.0	720.0	744.0	744.0
	2017	332.0	283.0	201.0	222.0
	2018	744.0	449.0	274.0	141.0
Total Air Flow (m³/h)	2016	121,344.6	112,654.7	115,274.9	107,644.8
	2017	49,690.8	40,996.5	28,225.3	32,077.2
	2018	107,924.5	62,524.7	38,119.5	19,595.9

The number of GAHE operating hours during which air was cooled deserves closer inspection. The number of hours when air was cooled by the GAHE accounted for 27% of total operating hours in 2016, 39% in 2017, and 51% in 2018. In the theoretical model with the same number of operating hours, the number of hours when air was cooled accounted for 58% of total operating hours in 2016, 73% in 2017, and 84% in 2018. A comparison of real-world data with the modeled values revealed considerable differences in GAHE performance across the years.

In Figure 5, the difference in air temperature between the GAHE inlet and outlet was plotted against the temperature of ambient air based on real-world data and modeled data. The trend lines for modeled data have a smaller slope than the trend lines for experimental data. During the conducted measurements, air was cooled only when outdoor temperature reached 15.8 °C in 2016 and 16.7 °C in successive years, whereas in the theoretical model, air was cooled already at an ambient temperature of 5.5 °C in 2016 and 2018, and 5.1 °C in 2017. Based on the measured data, air ceased to be preheated by the GAHE when ambient temperature exceeded 22.3 °C in 2016, 20.9 °C in 2017, and 22.6 °C in 2018. According to the model, the GAHE ceased to preheat air when outdoor temperature was higher than 19.2 °C in 2016, 16.9 °C in 2017, and 18.6 °C in 2018.
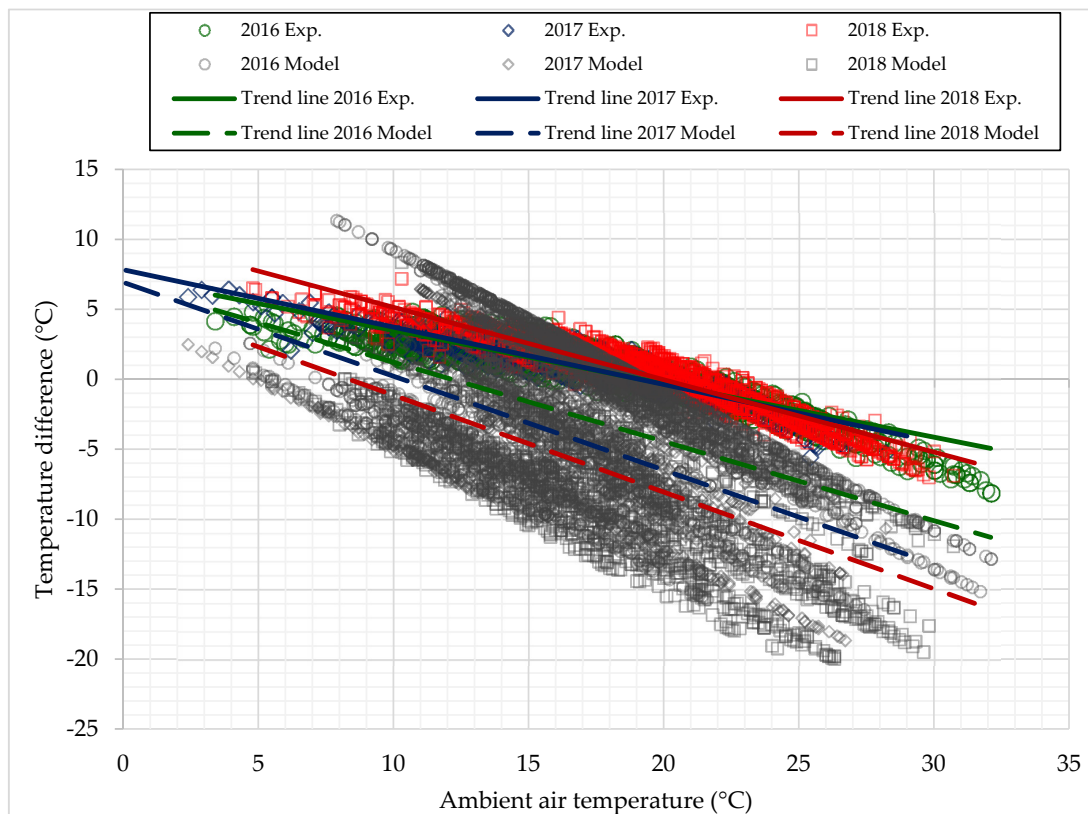

Figure 5. Differences in air temperature between the GAHE inlet and outlet (real-world and modeled data) relative to ambient air temperature.

The model produced a better fit to the experimental data in an analysis of monthly energy gain per 1 m³/h of flowing air (Figure 6). In general, heat gain was higher in the experiment than in the theoretical model. In all years of the study, the heat gain determined in the experiment was 98% higher in May and 77% higher in June than that calculated in the theoretical model. In July 2017 and 2018, heat gain was only around 30% higher in the experiment than in the model. In the remaining four months, theoretical heat gain was higher than the experimentally determined heat gain. In July 2016, August 2016, and August 2017, the modeled heat gain was approximately twice higher than that determined in the experiment.
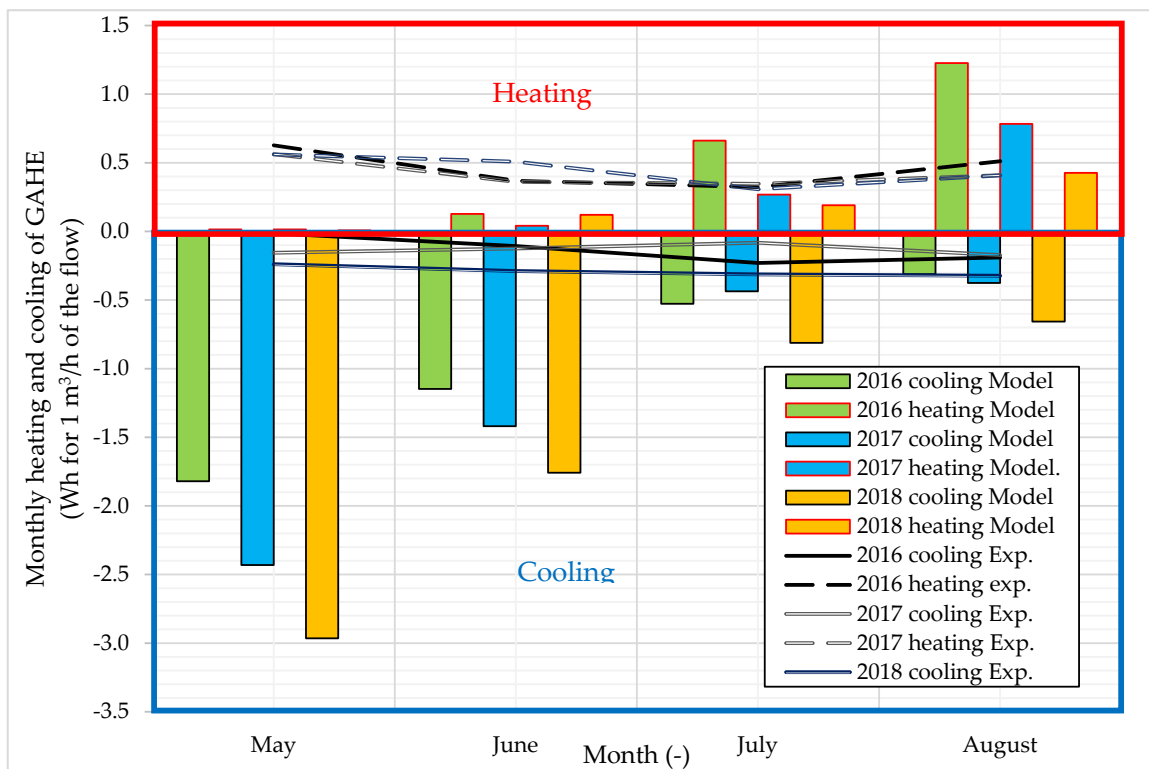

Figure 6. Monthly heating and cooling loads of the GAHE (Wh per 1 m³/h of flowing air).

The monthly cooling load (Figure 6) was clearly higher in the model than in the experiment. The difference between modeled and experimental data decreased gradually in successive months of each analyzed year. The theoretical cooling load was 130 times higher than the experimentally determined cooling load in May 2016. The modeled values were 11-fold higher than the experimental values in June 2016, and twice higher in August 2016. In 2017, the theoretical load was 16 times higher in May, 11 times higher in June, 5 times higher in July, and 2 times higher in August than that measured in the experiment. The theoretical and the experimental values were most consistent in 2018 when the modeled cooling load exceeded the experimentally determined load 12-fold in May, 3-fold in June, and 2-fold in July and August.

An analysis of hourly heating and cooling loads of the GAHE is presented in Table 2. The number of operating hours differed across the analyzed years. The GAHE operated continuously (2952 h) in 2016 and intermittently in the remaining years of the experiment. The total number of operating hours was 1038 in 2017 and 1608 in 2018. Based on the experimental data for 2016, the highest hourly heating and cooling loads were determined at 259.9 Wh and −108.6 Wh, respectively, in May; 204.0 Wh and −317.7 Wh, respectively, in June; 211.6 Wh and −401.9 Wh, respectively, in July; 231.3 Wh and −409.7 Wh, respectively, in August. The experimental data for 2017 revealed maximum hourly heating and cooling loads of 317.6 Wh and −240.4 Wh, respectively, in May; 172.5 Wh and −233.7 Wh, respectively, in June; 211.1 Wh and −153.9 Wh, respectively, in July; 171.7 Wh and −470.8 Wh, respectively, in August.

Based on the experimental data for 2018, the highest hourly heating and cooling loads were determined at 328.1 Wh and −326.0 Wh, respectively, in May; 294.4 Wh and −327.2 Wh, respectively, in June; 193.5 Wh and −311.6 Wh, respectively in July; 335.9 Wh and −340.1 Wh, respectively, in August.

Table 2. Distribution of hourly heating and cooling loads of the GAHE (Wh).

Heating and Cooling Loads of the GAHE (Wh)	Hours with Specific Heating and Cooling Loads of the GAHE (Number)					
	2016		**2017**		**2018**	
	Exp.	Model	Exp.	Model	Exp.	Model
−950	0	0	0	0	0	2
−900	0	0	0	0	0	13
−850	0	1	0	2	0	19
−800	0	8	0	7	0	23
−750	0	2	0	9	0	30
−700	0	20	0	6	0	47
−650	0	22	0	12	0	39
−600	0	34	0	17	0	57
−550	0	47	0	13	0	67
−500	0	70	0	25	0	65
−450	0	78	1	29	0	63
−400	4	95	0	31	0	80
−350	13	115	0	61	0	89
−300	17	133	0	66	7	104
−250	15	168	2	77	22	110
−200	30	160	14	93	66	138
−150	57	173	24	85	76	105
−100	97	206	33	79	112	109
−50	152	210	76	80	111	79
0	251	180	144	70	155	107
50	548	197	220	82	235	104
100	825	185	259	47	302	54
150	653	182	164	39	271	45
200	236	150	61	39	154	32
250	52	148	28	32	70	17
300	4	131	10	18	23	6
350	0	105	2	18	3	2
400	0	72	0	1	0	0
450	0	42	0	0	0	1
500	0	10	0	0	0	0
550	0	3	0	0	0	0

A comparison of hourly heating and cooling loads based on the experimental and the modeled data revealed a much higher number of hours with a heating load of 50–200 Wh (in particular in 2016) during the experiment. In turn, the number of hours with a cooling load below −450 Wh or a heating load above 350 Wh was higher in the theoretical model, and the above values were never exceeded in the experiment. The above values accounted for 18% of the modeled values in 2016, around 13% of the modeled values in 2017, and around 27% of the modeled values in 2018. Based on the modeled data for 2016, the highest hourly heating and cooling loads were determined at 179.6 Wh and −857.2 Wh, respectively, in May; 258.9 Wh and −841.0 Wh, respectively, in June; 399.0 Wh and −736.1 Wh, respectively, in July; 591.9 Wh and −587.9 Wh, respectively in August. The modeled data for 2017 revealed that the highest hourly heating and cooling loads reached 164.8 Wh and −864.9 Wh, respectively, in May; 115.4 Wh and −617.3 Wh, respectively in June; 275.0 Wh and −333.6 Wh, respectively, in July; 351.5 Wh and −460.8 Wh, respectively, in August. Based on the modeled data for 2018, the highest hourly heating and cooling loads were determined at 82.0 Wh

and −981.0 Wh, respectively in May; 296.5 Wh and −822.0 Wh, respectively, in June; 290.2 Wh and −477.8 Wh, respectively in July; 432.2 Wh and −518.1 Wh, respectively, in August.

The cooling load of a GAHE is also related to moisture condensation which is calculated with the use of formulas (8) and (9). A comparison of sensible and latent cooling capacity in 2018 is presented in Table 3.

Table 3. Total cooling capacity, sensible cooling capacity, and latent cooling capacity of the GAHE in 2018

		Sensible Cooling Capacity (Wh)		Latent Cooling Capacity (Wh)		Total Cooling Capacity (Wh)	
		Hourly	Daily	Hourly	Daily	Hourly	Daily
May	Avg.	−110.8	−832.6	−80.7	−604.3	−129.1	−1649.7
	Max.	−1.0	0.0	−0.7	0.0	−0.7	−17.5
	Min.	−326.0	−3056.7	−378.6	−2335.4	−564.1	−5035.4
	Total	−25,810.9		−18,731.9		−44,542.8	
June	Avg.	−127.4	−603.0	−92.5	−419.5	−163.2	−1704.2
	Max.	−1.0	0.0	−0.8	0.0	−0.8	−12.5
	Min.	−327.2	−2625.9	−573.8	−3146.9	−661.0	−4962.7
	Total	−18,089.3		−12,586.1		−30,675.4	
July	Avg.	−97.0	−385.0	−134.1	−558.1	−173.0	−1827.1
	Max.	−1.9	0.0	−0.9	0.0	−2.4	−331.0
	Min.	−311.6	−1445.5	−660.6	−4132.0	−903.6	−5577.6
	Total	−11,934.1		−17,299.7		−29,233.9	
August	Avg.	−135.0	−204.7	−145.2	−154.6	−218.4	−928.1
	Max.	−1.9	0.0	−5.6	0.0	−14.6	−50.0
	Min.	−340.1	−1128.5	−432.3	−1475.8	−624.6	−2105.0
	Total	−6345.6		−4791.4		−11,137.0	

In 2018, sensible cooling capacity and latent cooling capacity were estimated at −25.8 kWh and −18.7 kWh, respectively, in May; −18.8 kWh and −12.6 kWh, respectively, in June; −11.9 kWh and −17.3 kWh, respectively, in July; −6.3 kWh and −4.8 kWh, respectively, in August. Total cooling capacity reached −115.6 kWh, where sensible cooling capacity accounted for 54% and latent cooling capacity – for 46% of the overall energy balance.

4. Discussion

The performance of a GAHE was analyzed between May and August of 2016, 2017, and 2018. In the studied period, air temperature, and solar irradiance continued to increase relative to TMY data as well as previous year's data. The warmest year was 2018 when the number of hours with temperatures above 25 °C was considerably higher than in the remaining years of the study. The number of hours with the lowest temperatures (below 12 °C) which generally occur in spring also continued to decrease. Sub-zero temperatures, which appear in the TMY dataset, were not encountered during the study. Although the measurements were conducted over a period of only three years which were not too distant from the period covered by the TMY dataset (1971–2000), the recorded data are indicative of climate change and global warming. The above observation is supported by the discrepancies between the experimentally measured and modeled temperatures at the GAHE outlet. The differences between the experimental and modeled values of average monthly temperature at the GAHE outlet reached 7.1 °C to 9.6 °C in May, 3.8 °C to 5.5 °C in June, 0.1 °C to 1.3 °C in July, and 0.4 °C to 1.8 °C in August. The temperatures calculated in the theoretical model were below the experimental values in the spring of each year. The modeled values were characterized by a better fit to the experimental data in summer (July and August). In the analyzed period, the GAHE was able to increase or decrease the average hourly temperature of outdoor air by up to 7.1 °C and 8.1 °C, respectively. However, the operating time

of the GAHE differed in each year of the experiment. In 2016, the GAHE operated continuously, but outdoor air was precooled during only 27% of total operating time. The above can be attributed to the accumulation of heat around exchanger tubes in the ground when the GAHE remained in continuous operation mode. In the two remaining years, the GAHE operated intermittently, and outdoor air was precooled during 39% and 51% of total operating time in 2017 and 2018, respectively. The cooling load was highest in 2018 which was the warmest year and the year in which the GAHE operated intermittently. Therefore, the thermal energy content of soil was able to regenerate when the GAHE was not operating. However, according to the theoretical model, the number of hours during which outdoor air was precooled should be higher (72% on average in all years), in particular in spring, when low ground temperature after winter should support effective air cooling.

The observed discrepancies between the measured and the modeled values were also reflected in the GAHE's heating and cooling loads. According to the model, the GAHE should primarily cool outdoor air in May and June. However, the measured values indicate that air was mostly heated during that period, and the experimentally derived cooling loads were similar in all months. Both the experimental and the modeled values indicate that cooling loads should be higher in warmer years (2018) and that heating loads should be higher in colder years (2016). These observations clearly suggest that GAHEs should be popularized in an era of climate change.

Based on the conducted measurements, the annual heating load of the GAHE was determined at 210 kWh in 2016, 66 kWh in 2017, and 112 kWh in 2018. The corresponding values in the theoretical model were 224 kWh, 35 kWh, and 24 kWh. The sensible cooling load (negative values) was determined at −61 kWh in 2016, −21 kWh in 2017, and −62 kWh in 2018 based on the experimentally derived values, and at −444 kWh, −203 kWh, and −474 kWh, respectively, based on the modeled values. However, it should be noted that latent cooling capacity accounts for a high percentage of total cooling capacity (up to 50%).

5. Conclusions

The theoretical temperature at the GAHE outlet was directly influenced by the type of the model for calculating temperature distribution in the ground. Various models have been proposed in the literature. The authors selected a model based on PN-EN 16798-5 1:2017-07 to verify the extent to which this European standard is consistent with the experimentally determined temperature at the GAHE outlet in northeastern Poland.

The theoretical mathematical model applied in this study is easy to use, does not require specialist software, and can be implemented in early stages of designing HVAC systems in buildings. The values generated by the theoretical model based on Standard PN-EN 16798-5 1:2017-07 were relatively consistent with the experimentally measured data in summer, whereas considerable discrepancies between the modeled values and real-life measurements were observed in the transitional period (spring).

Further research is needed to verify the results of this study. The performance of the GAHE in fall and winter will be analyzed in an upcoming study. The volume of the experimentally measured and simulated data exceeds manuscript length limits; therefore, fall/winter data will be presented in a separate article. The performance of the GAHE will be analyzed in all months of the year, and the results will be used to optimize the theoretical mathematical model proposed by Standard PN-EN 16798-5 1:2017-07 to obtain a better fit with the experimental data.

Conflicts of Interest: The authors declare no conflicts of interest.

References

1. Carlucci, S.; Cattarin, G.; Pagliano, L.; Pietrobon, M. Optimization of the Installation of an Earth-to-Air Heat Exchanger and Detailed Design of a Dedicated Experimental Set-up. In *Applied Mechanics and Materials*; Trans Tech Publications: Switzerland, 2014; Volume 501, pp. 2158–2161.

2. Choudhury, T.; Misra, A.K. Minimizing changing climate impact on buildings using easily and economically feasible earth to air heat exchanger technique. *Mitig. Adapt. Strateg. Glob. Chang.* **2014**, *19*, 947–954. [CrossRef]

3. Tan, L.; Love, J. A literature review on heating of ventilation air with large diameter earth tubes in cold climates. *Energies* **2013**, *6*, 3734–3743. [CrossRef]

4. Skotnicka-Siepsiak, A.; Wesołowski, M.; Piechocki, J. Validating Models for Calculating the Efficiency of Earth-to-Air Heat Exchangers Based on Laboratory Data for Fall and Winter 2016 in Northeastern Poland. *Pol. J. Environ. Stud.* **2019**, *28*. [CrossRef]

5. PN-EN 15241:2011. *Wentylacja Budynków—Metody Obliczania Strat Energii w Budynkach Spowodowanych Wentylacją i Infiltracją Powietrza*; PKN: Warszawa, Poland, 2011.

6. Popiel, C.O.; Wojtkowiak, J. Temperature distributions of ground in the urban region of Poznan City. *Exp. Therm. Fluid Sci.* **2013**, *51*, 135–148. [CrossRef]

7. Morshed, W.; Leso, L.; Conti, L.; Rossi, G.; Simonini, S.; Barbari, M. Cooling performance of earth-to-air heat exchangers applied to a poultry barn in semi-desert areas of south Iraq. *Int. J. Agric. Biol. Eng.* **2018**, *11*, 47–53. [CrossRef]

8. Sobti, J.; Singh, S.K. Earth-air heat exchanger as a green retrofit for Chandīgarh—A critical review. *Geotherm. Energy* **2015**, *3*, 1–9. [CrossRef]

9. Sehli, A.; Hasni, A.; Tamali, M. The potential of earth-air heat exchangers for low energy cooling of buildings in South Algeria. *Energy Procedia* **2012**, *18*, 496–506. [CrossRef]

10. Wengang, H.; Yanhua, L.; Mingxin, L. Application of earth-air heat exchanger cooling technology in an office building in Jinan city. *Energy Procedia* **2019**, *158*, 6105–6111. [CrossRef]

11. Ozgener, L. A review on the experimental and analytical analysis of earth to air heat exchanger (EAHE) systems in Turkey. *Renew. Sustain. Energy Rev.* **2011**, *15*, 4483–4490. [CrossRef]

12. Estrada, E.; Labat, M.; Lorente, S.; Rocha, L.A. The impact of latent heat exchanges on the design of earth air heat exchangers. *Appl. Therm. Eng.* **2018**, *129*, 306–317. [CrossRef]

13. Bordoloi, N.; Sharma, A.; Nautiyal, H.; Goel, V. An intense review on the latest advancements of Earth Air Heat Exchangers. *Renew. Sustain. Energy Rev.* **2018**, *89*, 261–280. [CrossRef]

14. Agrawal, K.K.; Misra, R.; Agrawal, G.D.; Bhardwaj, M.; Jamuwa, D.K. The state of art on the applications, technology integration, and latest research trends of earth-air-heat exchanger system. *Geothermics* **2019**, *82*, 34–50. [CrossRef]

15. Soltani, M.; Kashkooli, F.M.; Dehghani-Sanij, A.R.; Kazemi, A.R.; Bordbar, N.; Farshchi, M.J.; Elmi, K.; Gharali, M.; Dusseault, M.B. A comprehensive study of geothermal heating and cooling systems. *Sustain. Cities Soc.* **2019**, *44*, 793–818. [CrossRef]

16. Misra, A.K.; Gupta, M.; Lather, M.; Garg, H. Design and performance evaluation of low cost Earth to air heat exchanger model suitable for small buildings in arid and semi arid regions. *KSCE J. Civ. Eng.* **2015**, *19*, 853–856. [CrossRef]

17. Baglivo, C.; D'Agostino, D.; Congedo, P. Design of a ventilation system coupled with a horizontal air-ground heat exchanger (HAGHE) for a residential building in a warm climate. *Energies* **2018**, *11*, 2122. [CrossRef]

18. Wang, S.H.; Sheng, C.; Chou, H.M.; Corado, E.J.T. A Study of Solar Panel Chimney for House Ventilation. In *Applied Mechanics and Materials*; Trans Tech Publications: Switzerland, 2013; Volume 422, pp. 118–122.

19. Liu, Q.; Du, Z.; Fan, Y. Heat and Mass Transfer Behavior Prediction and Thermal Performance Analysis of Earth-to-Air Heat Exchanger by Finite Volume Method. *Energies* **2018**, *11*, 1542. [CrossRef]

20. Congedo, P.; Lorusso, C.; De Giorgi, M.; Marti, R.; D'Agostino, D. Horizontal air-ground heat exchanger performance and humidity simulation by computational fluid dynamic analysis. *Energies* **2016**, *9*, 930. [CrossRef]

21. Agrawal, K.K.; Bhardwaj, M.; Misra, R.; Agrawal, G.D.; Bansal, V. Optimization of operating parameters of earth air tunnel heat exchanger for space cooling: Taguchi method approach. *Geotherm. Energy* **2018**, *6*, 10. [CrossRef]

22. Kumar, R.; Sinha, A.R.; Singh, B.K.; Modhukalya, U. A design optimization tool of earth-to-air heat exchanger using a genetic algorithm. *Renew. Energy* **2008**, *33*, 2282–2288. [CrossRef]

23. Ahmed, S.F.; Amanullah, M.T.O.; Khan, M.M.K.; Rasul, M.G.; Hassan, N.M.S. Parametric study on thermal performance of horizontal earth pipe cooling system in summer. *Energy Convers. Manag.* **2016**, *114*, 324–337. [CrossRef]

24. Rodrigues, M.K.; da Silva Brum, R.; Vaz, J.; Rocha, L.A.O.; dos Santos, E.D.; Isoldi, L.A. Numerical investigation about the improvement of the thermal potential of an Earth-Air Heat Exchanger (EAHE) employing the Constructal Design method. *Renew. Energy* **2015**, *80*, 538–551. [CrossRef]

25. Bisoniya, T.S. Design of earth–air heat exchanger system. *Geotherm. Energy* **2015**, *3*, 18. [CrossRef]

26. Rouag, A.; Benchabane, A.; Mehdid, C.E. Thermal design of Earth-to-Air Heat Exchanger. Part I a new transient semi-analytical model for determining soil temperature. *J. Clean. Prod.* **2018**, *182*, 538–544. [CrossRef]

27. Mehdid, C.E.; Benchabane, A.; Rouag, A.; Moummi, N.; Melhegueg, M.A.; Moummi, A.; Benabdi MLBrima, A. Thermal design of Earth-to-air heat exchanger. Part II a new transient semi-analytical model and experimental validation for estimating air temperature. *J. Clean. Prod.* **2018**, *198*, 1536–1544. [CrossRef]

28. Chiesa, G. EAHX–Earth-to-air heat exchanger: Simplified method and KPI for early building design phases. *Build. Environ.* **2018**, *144*, 142–158. [CrossRef]

29. Peretti, C.; Zarrella, A.; De Carli, M.; Zecchin, R. The design and environmental evaluation of earth-to-air heat exchangers (EAHE). A literature review. *Renew. Sustain. Energy Rev.* **2013**, *28*, 107–116. [CrossRef]

30. Kusuda, T.; Achenbach, P.R. *Earth Temperature and Thermal Diffusivity at Selected Stations in the United States*; (No. NBS-8972); National Bureau of Standards: Gaithersburg, MD, USA, 1965.

31. Phetteplace, G.; Bahnfleth, D.; Mildenstein, P.; Overgaard, J.; Rafferty, K.; Wade, D.W. *District Heating Guide*; ASHRAE: Atlanta, GA, USA, 2013.

32. Tittelein, P.; Achard, G.; Wurtz, E. Modelling earth-to-air heat exchanger behaviour with the convolutive response factors method. *Appl. Energy* **2009**, *86*, 1683–1691. [CrossRef]

33. Badache, M.; Eslami-Nejad, P.; Ouzzane, M.; Aidoun, Z.; Lamarche, L. A new modeling approach for improved ground temperature profile determination. *Renew. Energy* **2016**, *85*, 436–444. [CrossRef]

34. Ozgener, O.; Ozgener, L.; Tester, J.W. A practical approach to predict soil temperature variations for geothermal (ground) heat exchangers applications. *Int. J. Heat Mass Transf.* **2013**, *62*, 473–480. [CrossRef]

35. Awadukt Thermo Ground-Air Heat Exchanger Renewable Cooling Solution for Low Energy Buildings. Available online: https://www.rehau.com/download/1420434/sales-brochure.pdf (accessed on 24 March 2020).

36. Liu, Z.; Yu, Z.J.; Yang, T.; Li, S.; El Mankibi, M.; Roccamena, L.; Qi, D.; Zhang, G. Designing and evaluating a new earth-to-air heat exchanger system in hot summer and cold winter areas. *Energy Procedia* **2019**, *158*, 6087–6092. [CrossRef]

37. Li, H.; Ni, L.; Yao, Y.; Sun, C. Experimental investigation on the cooling performance of an Earth to Air Heat Exchanger (EAHE) equipped with an irrigation system to adjust soil moisture. *Energy Build.* **2019**, *196*, 280–292. [CrossRef]